TWMS J. App. and Eng. Math. V.16, N.6, 2026, pp.808-823

A UNIFIED SPECTRAL FILTER FRAMEWORK FOR ILL-POSED LINEAR OPERATOR EQUATIONS IN HILBERT SPACES

B. BHASKAR REDDY[1*], RAJA KUMARI CHILUKURI[2], ANIL CHOWDARY TUMMALA[3], VENKATESWARA RAO MUSALA[4], HARI KISHORE KAKARLA[5], KAVITHA MANOHARAN[6], §

Abstract. Regularization is useful for stable recovery in inverse problems with ill-posed linear operator equations in Hilbert spaces because small perturbations in data can make problems highly unstable. Tikhonov regularization, truncated singular value decomposition, and iterative polynomial filtering, classical methods, have been understood from singular value decay and the Picard condition. However, most literature analyses convergence, parameter choice, and saturation from separate perspectives. This study fills the gap by constructing a unified spectral filter framework that integrates bias–variance decomposition, polynomial and exponential decay, convergence rate analysis, and stability-consistent parameter choice frameworks, including the discrepancy principle and the L-curve criterion. To enhance saturation control and qualification, we propose extensions to fractional and generalized spectral filters. In the severely ill-posed setting, we identify logarithmic convergence barriers with the inductive method, thereby exposing accuracy limits that exist independently from filter design. The findings are directly applicable to stable inversion and are operator theoretically sound for real-world applications, including medical imaging, geophysical reconstruction, signal processing, and data-driven recovery of ill-conditioned systems.

Keywords: ill-posed operator equations; Hilbert spaces; spectral regularization; Tikhonov regularization; truncated SVD; iterative methods.

AMS Subject Classification: 47A52

[1] Department of ECE, K.S.R.M. College of Engineering, Kadapa, A.P. India.
[2] Department of ECE, VNR Vignana Jyothi Institute of Engineering and Technology, Hyderabad, India.
[3] SRK Institute of Technology, Vijayawada, India.
[4] Department of ECE, Dhanekula Institute of Engineering and Technology, Vijayawada, India
[5] Department of ECE, Koneru Lakshmaiah Education Foundation (Deemed to be University), Vaddeswaram, Guntur, India.
[6] Department of ECE, Saveetha School of Engineering, Chennai, India.
e-mail: bhaskarbada@ksrmce.ac.in; ORCID no. 0000-0002-3200-0182 .
e-mail:rajakumari_ch@vnrvjiet.in; ORCID no. 0000-0002-0793-133X
e-mail:anilctummala5@gmail.com; ORCID no. 0000-0002-7115-8214
e-mail: venkatmusala@gmail.com; ORCID no. 000-0002-9404-8202
e-mail: kakarla.harikishore@kluniversity.in; ORCID no. 0000-0003-2622-3483
e-mail: Kavithavlsime@gmail.com; ORCID no. 0000-0001-9054-1449
[*] Corresponding author
§ Manuscript received: May 20, 2025; accepted: December 15, 2026.
TWMS Journal of Applied and Engineering Mathematics, Vol.16, No.6;

1. Introduction

Within the sphere of applied mathematics and modern analysis, the mathematical theory of inverse problems has rapidly developing fundamentals and offers new challenges. Scientific fields, particularly medical imaging, geophysical exploration, signal reconstruction, non-destructive evaluation, and parameter estimation of partial differential equations, are utilizing new theory and computations to solve problems associated with retrieving partially concealed structures via indirect measurements. Forward models are typically well-structured and stable, whereas inverse reconstruction processes are typically unstable. Much of the current literature focuses on this instability, stating that the instability an inverse problem presents is not a numerical one but a structural one and that this instability is a result of the underlying operator equations [1, 2, 3].

The modern theory on ill-posedness focuses on a solution's continuous dependence on data, or the lack of it. Even when existence or uniqueness is proven, reconstructed solutions may still diverge under small measurement perturbations. Recent operator-theoretic analyses attribute such instabilities to operator compactness and spectral decay [4, 5, 6]. These findings show that inverse problem theory in infinite-dimensional spaces differs fundamentally from finite-dimensional linear systems and therefore requires specific regularization strategies. In the Hilbert space framework, inverse problems are written as equations involving linear operators in infinite-dimensional spaces. An unknown element is mapped by a forward operator to data, and the character of the inverse problem depends on the analytical properties of this operator. If the operator is compact, the inverse, if it exists formally, must be unbounded. By studying singular value distributions and the operator range structure, the ill-posedness of such problems can be classified more precisely [7, 8, 9]. These spectral properties form the foundation of regularization theory.

The degree to which a problem is ill-posed is determined by the speed of singular value decay. Polynomial decay is considered mild, while exponential decay is considered more severe. Contemporary analyses have studied the impact of such spectral characteristics on convergence rates and reconstruction accuracy [10, 11, 12]. Measurements are always accompanied by noise due to modeling error, discretization, or random noise, and recent studies have pointed out how reconstruction stability should be analyzed with respect to specific noise models and perturbation bounds [3, 13]. Without sufficient stabilization, inversion processes enhance noise affecting the small singular values of the data, producing reconstructions that are unable to provide useful information [4, 14].

Regularization offers one of the primary methods to increase stability. Instead of directly inverting the operator, one creates a sequence of stable approximations to the inverse determined by a regularization constant. Recent works have shown that classical Tikhonov-type frameworks can be generalized to include multi-penalty, fractional, and hybrid regularization [3, 5, 15]. Modifications to regularized iterative techniques, including Landweber and Newton-type methods, have also been made to enhance convergence rates and stability for large-scale problems [2, 16].

Recent spectral filtering methods provide a useful way of unifying mechanisms across disciplines. From this viewpoint, each method corresponds to a spectral filtering operator, where unstable components are reduced while stable modes are conserved. Recent theoretical studies have clarified that filter functions determine convergence, saturation behavior, and noise robustness [6, 8, 17]. Another important element of regularization theory is parameter choice, and recent research has focused on the discrepancy principle, adaptive parameters, and hybrid selection methods in which analytical and data-driven methodologies are combined [4, 10, 18]. In a broader computational context, learning-enhanced predictive frameworks have also shown that integrating structured representations with optimization-based tuning can improve model reliability under complex data conditions [5]. The relationship between theoretical convergence rates and practical parameter selection continues to be a central concern in the inverse problem community [1, 19].

The most recent literature suggests that classical, generalized, and fractional regularization techniques, together with extended spectral filtering, still face limitations due to saturation phenomena, which restrict convergence rates even when the underlying solution has higher-order smoothness [3, 15, 20]. The Hilbert space environment remains especially useful for analyzing these effects, as its geometry supports the formulation of estimates and convergence rates. Recent research also emphasizes operator-based analysis of learning-based regularization and hybrid iterative methods [9, 16], whose integration with classical functional analysis further strengthens regularization theory in Hilbert spaces. The main aim of this paper is to provide an analytically complete study of regularization techniques for ill-posed linear operator equations in Hilbert spaces. It examines spectral descriptions of ill-posedness, compares classical and modern regularization methods, discusses parameter choice strategies, and studies asymptotic convergence, with emphasis on how operator compactness and spectral decay affect reconstruction quality. Subsequent sections elaborate on spectral analysis, compare regularization methods, and discuss stability and convergence under a range of structural assumptions.

2. Spectral Characterization and Picard Condition Analysis

The roots of the instability of inverse problems in Hilbert spaces lie in determining the spectrum of the forward operator. Unlike finite-dimensional linear systems, singular values of compact operators in infinitely-dimensional spaces accumulate at zero. This mechanism of spectral collapse is the primary cause of ill-posedness. This section builds the spectral theory of compact operators and explains the Picard condition in the solvability and stability framework.

The linear operator $A : \mathcal{H}_1 \to \mathcal{H}_2$ is compact. In the separable Hilbert spaces, we have the singular value decomposition theorem, which gives orthonormal systems $\{u_i\} \subset \mathcal{H}_2$ and $\{v_i\} \subset \mathcal{H}_1$, and a sequence of nonnegative singular values $\{\sigma_i\}$ such that

$$\sigma_1 \geq \sigma_2 \geq \sigma_3 \geq \cdots \to 0, \tag{2.1}$$

such that

$$Av_i = \sigma_i u_i, \quad A^* u_i = \sigma_i v_i. \tag{2.2}$$

This decomposition leads to the spectral expansion

$$Ax = \sum_{i=1}^{\infty} \sigma_i \langle x, v_i \rangle u_i, \tag{2.3}$$

converging in $\mathcal{H}_2$ for every $x \in \mathcal{H}_1$. The forward mapping defined in (2.3) is continuous, and while this is true the inverse mapping is unconstrained when $\sigma_i \to 0$ [23].

The singular value sequence describes the extent and nature of ill-posedness [3]. For many inverse problems related to some smoothing operator or integral equation, the sequence has either polynomial or exponential decay. Polynomial decay of the type

$$\sigma_i \sim i^{-p}, \quad p > 0, \tag{2.4}$$

represents mildly ill-posed problems, while the singular value decay of

$$\sigma_i \sim e^{-qi}, \quad q > 0, \tag{2.5}$$

describes severely ill-posed problems [7, 24]. These two types of singular value decay are shown in Figure 1.

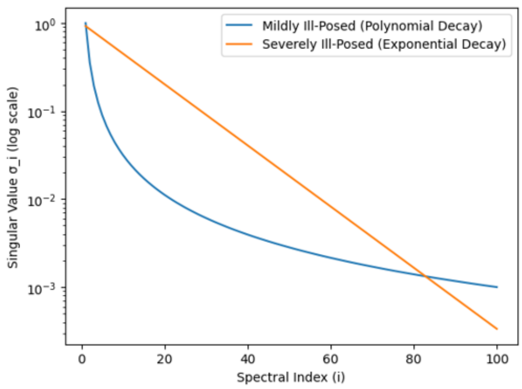

FIGURE 1. Singular Value Decay for Mildly and Severely Ill-Posed Operators

Formally, we have the operator of the equation

$$Ax = y \tag{2.6}$$

describing an operator being inverted, we can have the spectral description of the solution

$$x = \sum_{i=1}^{\infty} \frac{\langle y, u_i \rangle}{\sigma_i} v_i. \tag{2.7}$$

Expression (2.7) shows the source of the instability [21]. When $\sigma_i \to 0$, the factors $1/\sigma_i$ grow, especially at high spectral indices. Let us say the available data has been perturbed by

$$y^\delta = y + \delta\eta, \tag{2.8}$$

where $\delta > 0$ represents the magnitude of noise, and η is a disturbance with unit norm. Plugging (2.8) into (2.7) gives:

$$x^\delta = \sum_{i=1}^{\infty} \frac{\langle y, u_i \rangle}{\sigma_i} v_i + \delta \sum_{i=1}^{\infty} \frac{\langle \eta, u_i \rangle}{\sigma_i} v_i. \tag{2.9}$$

Because the coefficients are divided by increasingly smaller singular values, the noise component dominates the expansion for large indices [8, 25]. Figure 2 demonstrates how the amplification factor $1/\sigma_i$ grows with the spectral index. The coherence between the

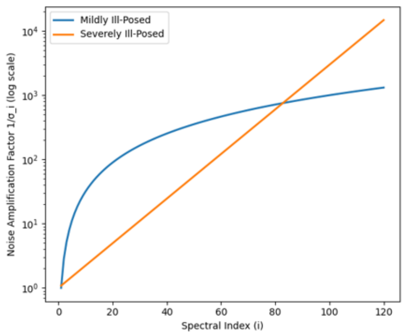

FIGURE 2. Instability of the Naïve Inverse: Noise Amplification vs Spectral Index

singular values and the data coefficients is formalized in the Picard condition [9]. A necessary and sufficient condition for the existence of a minimum-norm solution is given by

$$\sum_{i=1}^{\infty} \frac{|\langle y, u_i \rangle|^2}{\sigma_i^2} < \infty. \tag{2.10}$$

Condition (2.10) requires the spectral coefficients of the data to decay sufficiently fast relative to the singular values; otherwise, the series in (2.7) diverges. Figure 3 shows this through the Picard plot of σ_i and $|\langle y, u_i \rangle|$ against the index i, where noise causes the coefficient curve to level out beyond a certain spectral index [22]. Figure 4 compares polynomial and exponential decay, showing greater instability in the exponential case, where components beyond the transition point become noise-dominated and amplify error through the factor $1/\sigma_i$.

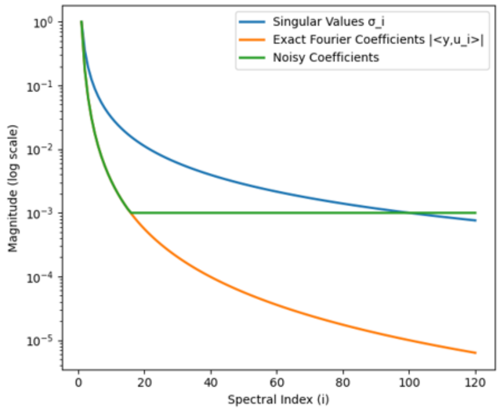

FIGURE 3. Picard Plot: Decay of Fourier Coefficients and Singular Values

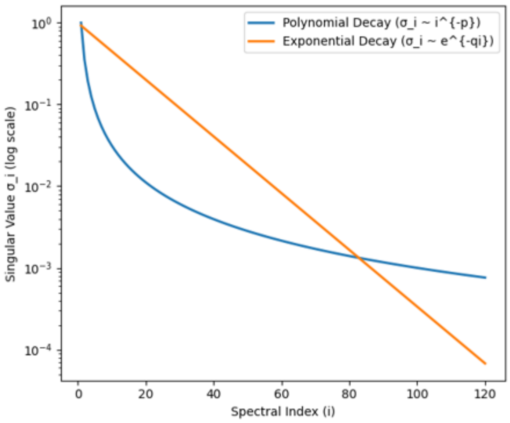

FIGURE 4. Comparison of Polynomial and Exponential Spectral Decay

The spectral analysis in this section shows that ill-posedness is linked to compactness and singular value decay [26]. The Picard condition describes the compatibility that must be present for a solution to exist, while the classification of mild and severe ill-posedness provides a measure of the extent to which the system can be unstable.

3. Classical Regularization Methods and Error Decomposition

The primary mathematical hindrance in inverse operator equations is not the lack of a formal inverse, but the loss of continuity of the inverse function when the forward operator is compact. Classical regularization techniques resolve this by constructing a de-parameterized family of bounded solution operators for which the user specifies a parameter that balances the trade-off between approximation and stability. Here, we look at the classical techniques through the unified spectral-filter framework and then examine the reconstruction error in terms of bias-type and variance-type components.

We state the regularized solution to be the response of a bounded linear operator corresponding to perturbed data. Thus we consider a parametric family of operators

$$R_\alpha : \mathcal{H}_2 \to \mathcal{H}_1, \tag{3.1}$$

and associate the calculated solution with

$$x_\alpha^\delta = R_\alpha y^\delta, \tag{3.2}$$

where y^δ is the noisy data and δ is a measure of the level of perturbation. The regularizing structural requirement is that regularization should recover exact solutions for exact data. This is expressed through

$$\lim_{\alpha \downarrow 0} R_\alpha(Ax) = x, \quad x \in \mathcal{H}_1. \tag{3.3}$$

It is mathematically practical to define the operator of "reconstruction"

$$T_\alpha := R_\alpha A, \tag{3.4}$$

so that (3.3) becomes an approximation-to-identity condition

$$T_\alpha \to I \text{ strongly as } \alpha \downarrow 0. \tag{3.5}$$

Stability is satisfied if

$$\| R_\alpha \| < \infty \text{ for each fixed } \alpha > 0. \tag{3.6}$$

In the context of Hilbert spaces, classical regularization can be viewed in terms of spectral damping. We therefore write

$$x_\alpha^\delta = \sum_{i=1}^{\infty} g_\alpha(\sigma_i) \langle y^\delta, u_i \rangle v_i, \tag{3.7}$$

where g_α is the filter and $\{u_i\}, \{v_i\}$ are the singular vectors and σ_i the singular values. The corresponding reconstruction operator acts diagonally in the singular basis,

$$T_\alpha x = \sum_{i=1}^{\infty} \phi_\alpha(\sigma_i) \langle x, v_i \rangle v_i, \tag{3.8}$$

where the damping factor is

$$\phi_\alpha(\sigma) := \sigma g_\alpha(\sigma). \tag{3.9}$$

For consistency in the noise-free limit,

$$\lim_{\alpha \downarrow 0} \phi_\alpha(\sigma) = 1 \quad (\sigma > 0). \tag{3.10}$$

In many classical schemes, stability is controlled by the growth of the filter. The third is data space residual governed by the complementary factor $1 - \phi_\alpha$. Figure 5 illustrates the functions $g_\alpha(\sigma)$ and $\phi_\alpha(\sigma)$ for several classical methodologies, showing how very high-index components are suppressed and very low-index components are approximately inverted.

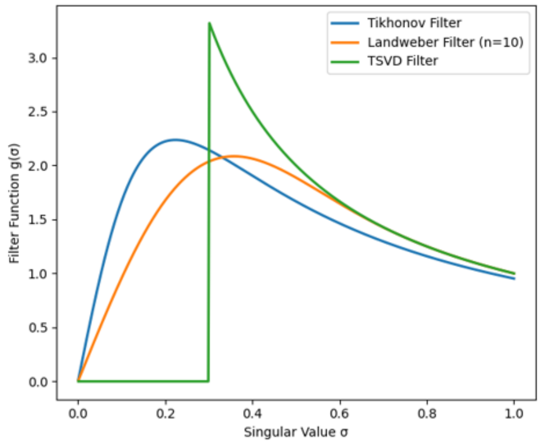

FIGURE 5. Spectral Filter Functions Associated with Regularization Schemes

We now consider Tikhonov regularization, the prototypical quadratic stabilization method for linear inverse problems in Hilbert spaces. Instead of attempting to solve $Ax = y^\delta$ directly, one looks for x_α^δ that is the minimizer of the penalized functional

$$\mathcal{J}_\alpha(x) = \| Ax - y^\delta \|^2 + \alpha \| x \|^2 . \tag{3.11}$$

The regularization parameter $\alpha > 0$ determines the balance between residual minimization and penalization of the norm. The first-order optimality condition delivers the normal equation

$$(A^*A + \alpha I)x_\alpha^\delta = A^* y^\delta. \tag{3.12}$$

As a consequence, an explicit representation for the regularization operator can be formed as follows:

$$R_\alpha = (A^*A + \alpha I)^{-1} A^*. \tag{3.13}$$

In the singular value decomposition, the method is applied via the scalar filter function

$$g_\alpha(\sigma) = \frac{\sigma}{\sigma^2 + \alpha}, \tag{3.14}$$

and therefore, the damping factor is

$$\phi_\alpha(\sigma) = \frac{\sigma^2}{\sigma^2 + \alpha}. \tag{3.15}$$

For large singular values, $g_\alpha(\sigma)$ behaves approximately like $1/\sigma$, while for small singular values the denominator dominates and controls amplification. The operator norm satisfies:

$$\| R_\alpha \| \leq \frac{1}{2\sqrt{\alpha}}. \tag{3.16}$$

These relations explain the classical bias–variance structure of Tikhonov regularization. For large α, the singular value filter suppresses small singular values, causing over smoothing and dominant approximation error. When α is too small, the amplification bound increases and significant noise is introduced into the solution. Figure 6 depicts this trade-off.

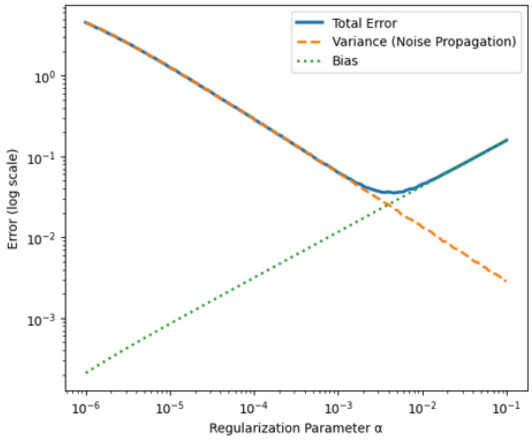

FIGURE 6. Bias–Variance Trade-Off in Tikhonov Regularization

The total error decomposition

$$x_\alpha^\delta - x^\dagger = (x_\alpha^\delta - x_\alpha) + (x_\alpha - x^\dagger). \tag{3.17}$$

The first term is the noise propagation term. Using (3.2) and (3.16),

$$\| x_\alpha^\delta - x_\alpha \| = \| R_\alpha (y^\delta - y) \| \leq \| R_\alpha \| \delta \leq \frac{\delta}{2\sqrt{\alpha}}. \tag{3.18}$$

The second term is the approximation error or bias. Using (3.8)-(3.9) and (3.15), the spectral bias satisfies

$$\| x_\alpha - x^\dagger \|^2 = \sum_{i=1}^{\infty} \left(\frac{\alpha}{\sigma_i^2 + \alpha} \right)^2 | \langle x^\dagger, v_i \rangle |^2, \tag{3.19}$$

which explains the bias-variance trade-off presented in Figure 6.

The Truncated Singular Value Decomposition (TSVD) controls instability differently through spectral truncation. Denote k as the truncation index, and define the truncated solution as

$$x_k^\delta = \sum_{i=1}^{k} \frac{\langle y^\delta, u_i \rangle}{\sigma_i} v_i. \tag{3.20}$$

TSVD can also be considered as the application of the filter

$$g_k(\sigma_i) = \begin{cases} 1/\sigma_i, & i \leq k, \\ 0, & i > k. \end{cases} \tag{3.21}$$

If k increases, the approximation improves, but stability reduces because the smallest retained singular values diminish and amplify noise. This balance is shown in Figure 7.

The total reconstruction error is described through a noise propagation term and a truncation bias term. Using the orthonormality of the singular vectors, we have

$$\| x_k^\delta - x_k \|^2 = \sum_{i=1}^{k} \frac{| \langle y^\delta - y, u_i \rangle |^2}{\sigma_i^2} \leq \delta^2 \sum_{i=1}^{k} \frac{1}{\sigma_i^2}. \tag{3.22}$$

The truncation bias describes the second term:

$$\| x_k - x^\dagger \|^2 = \sum_{i=k+1}^{\infty} | \langle x^\dagger, v_i \rangle |^2 . \tag{3.23}$$

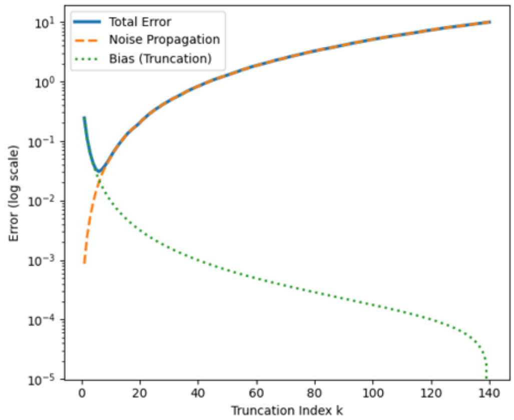

FIGURE 7. Error Behavior vs Truncation Index in TSVD

As k increases, this bias term decreases. TSVD may be viewed as the hard-cutoff analogue of Tikhonov smoothing.

Unlike other regularization approaches that rely on spectral modifications, iterative approaches use early stopping as their regularization mechanism. This is the classic semi-convergence behavior, where the reconstruction error, after initially decreasing as the dominant modes are captured, eventually increases as the noise-dominated modes are captured. This phenomenon is seen in Figure 8.

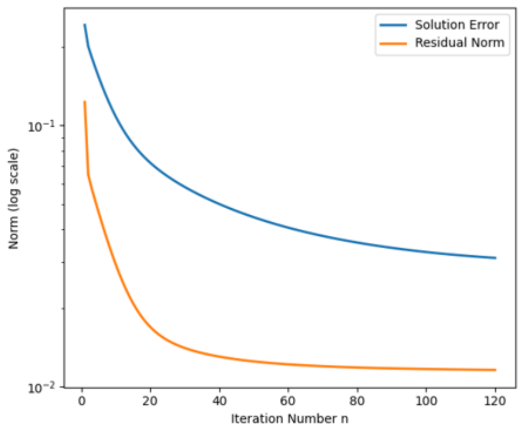

FIGURE 8. Convergence of Iterative Regularization Methods

In spectral form, the n-th iterate satisfies

$$x^{(n)} = \sum_{i=1}^{\infty} g_n(\sigma_i)\,\langle y^\delta, u_i\rangle\, v_i, \tag{3.24}$$

Landweber iteration induces a polynomial spectral filter whose shape depends on the iteration count. Early stopping therefore acts as a dynamic regularization parameter. The residual satisfies

$$\| Ax^{(n)} - y^\delta \|^2 = \sum_{i=1}^{\infty} (1 - \omega\sigma_i^2)^{2n} \mid \langle y^\delta, u_i\rangle \mid^2, \tag{3.25}$$

which shows that the data residual typically decreases as n increases. However, this does not guarantee monotone decrease of the solution error, as amplification of noise-dominated spectral components could happen at later iterations.

For any spectral regularization method, total error can be viewed in terms of the sum of a propagated noise term and an approximation term. Let $x^\dagger$ denote the exact solution. Then one can write

$$x_\alpha^\delta - x^\dagger = R_\alpha(y^\delta - y) + (T_\alpha - I)x^\dagger. \tag{3.26}$$

Considering norm, we get

$$\| x_\alpha^\delta - x^\dagger \| \leq \| R_\alpha \| \delta + \| (T_\alpha - I)x^\dagger \| . \tag{3.27}$$

If the filter is classically qualified, one can derive a bias estimate of the kind

$$\| (T_\alpha - I)x^\dagger \| \leq C\alpha^\mu. \tag{3.28}$$

Finally, combining these bounds, one obtains the classical trade-off

$$\| x_\alpha^\delta - x^\dagger \| \leq C\left(\alpha^\mu + \frac{\delta}{\sqrt{\alpha}}\right), \tag{3.29}$$

which analytically captures what is shown in Figure 6. Table 1 summarizes the main methods.

Table 1. Comparison of Classical Regularization Methods in Hilbert Spaces

Method	Regularized Solution Representation	Spectral Filter $g(\lambda)$, $\lambda = \sigma_i^2$	Stabilization Mechanism
Tikhonov Regularization	$x_\alpha^\delta = (A^*A + \alpha I)^{-1}A^*y^\delta$	$g_\alpha(\lambda) = \dfrac{1}{\lambda + \alpha}$	Smooth damping of small singular values
Truncated SVD (TSVD)	$x_k^\delta = \sum_{i=1}^{k} \dfrac{\langle y^\delta, u_i\rangle}{\sigma_i} v_i$	$g_k(\lambda_i) = \dfrac{1}{\lambda_i} 1_{i\leq k}$	Hard spectral cutoff at index k
Landweber Iteration (early stopping)	$x^{(n+1)} = x^{(n)} + \omega A^*(y^\delta - Ax^{(n)}), x^{(0)} = 0$	$g_n(\lambda) = \dfrac{1-(1-\omega\lambda)^n}{\lambda}$	Polynomial filtering via finite iteration
Iterated Tikhonov (order m)	$x_\alpha^{(m)} = (A^*A + \alpha I)^{-1}(A^*y^\delta + \alpha x_\alpha^{(m-1)}), x_\alpha^{(0)} = 0$	$g_\alpha^{(m)}(\lambda) = \dfrac{1}{\lambda}\left(1 - \left(\dfrac{\alpha}{\lambda+\alpha}\right)^m\right)$	Repeated smoothing with bias refinement

4. Results and Discussion: Parameter Choice Theory and Spectral Regularization Extensions

While the construction of bounded regularization operators offers stability on the operator scale, stability alone does not guarantee quality of reconstruction. A bounded operator prevents perturbations from growing uncontrollably, but this does not mean that the reconstructed solution will retain the essential structure of the unknown. For this reason, the regularization parameter becomes the main control mechanism in practical inversion. A regularization parameter that is too small reproduces the unstable inverse and allows noise to dominate the output. A parameter that is too large produces excessive smoothing and removes important features of the solution, thereby increasing bias. It is therefore appropriate to formulate parameter choice as the minimization of the total reconstruction error

$$\mathcal{E}(\alpha, \delta) = \| x_\alpha^\delta - x^\dagger \|, \tag{4.1}$$

where x_α^δ is the regularized solution associated with perturbed data and $x^\dagger$ is the actual solution.

The discrepancy principle is a classic rule based on the residual between the reconstructed data and the perturbed observation, and suggests selecting $\alpha = \alpha_\delta$ such that

$$r(\alpha_\delta) = \tau\delta, \quad \tau > 1. \tag{4.2}$$

This rule matches the residual to the noise level with a safety factor τ, avoiding overfitting while still respecting the data. Under suitable source conditions and stability assumptions, the regularized solution converges to the exact one. This mechanism is shown in Figure 9.

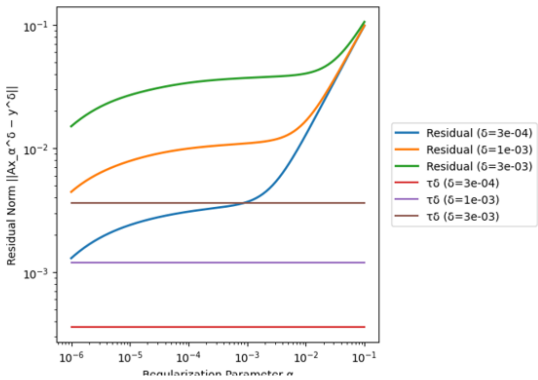

FIGURE 9. Discrepancy Principle: Residual Evolution vs Noise Level

When the noise level is not available, geometric parameter choice becomes attractive. The L-curve method examines the relation between the logarithm of the residual norm and the logarithm of the solution norm, which typically forms a corner separating high residual–low norm and low residual–high norm behavior. The optimal parameter is selected at the point of maximum curvature. Figure 10 shows this corner geometry.

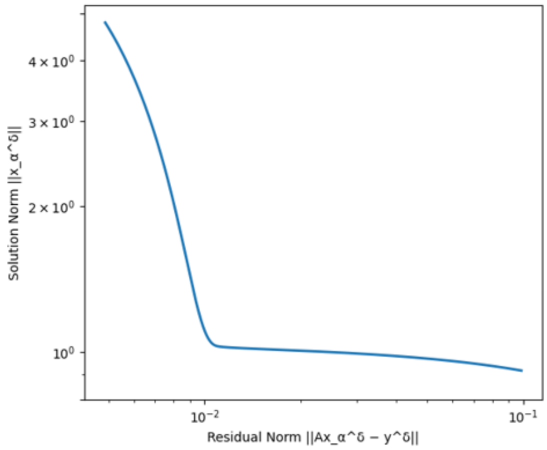

FIGURE 10. L-Curve Criterion: Residual Norm vs Solution Norm

Balancing the approximation and stability contributions leads to the scaling relation

$$\alpha_{opt} \asymp \delta^{\frac{1}{\mu+\nu}}, \tag{4.3}$$

which implies the optimal convergence rate

$$\mathcal{E}(\alpha_{opt}, \delta) \asymp \delta^{\frac{\mu}{\mu+\nu}}. \tag{4.4}$$

This shows that the optimal choice of the parameter leads to algebraic convergence rates resulting from the balance between the smoothness of the solution and the spectral decay. Figure 11 shows this scaling behavior numerically.

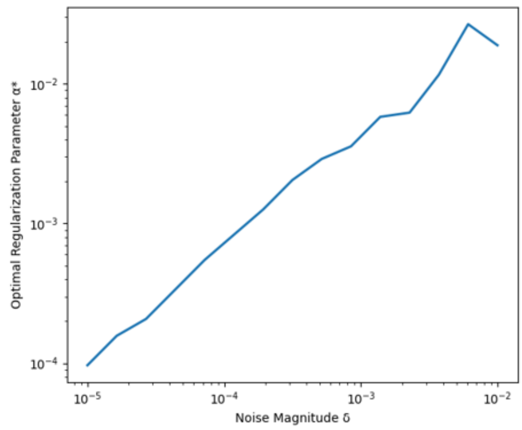

FIGURE 11. Optimal Regularization Parameter vs Noise Magnitude

Besides quadratic penalization, fractional spectral filters allow greater versatility in shaping the bias-stability trade-off. The additional parameter s adjusts the strength and profile of spectral attenuation, providing finer control of the balance between approximation and stability. Figure 12 shows that, for various fractional orders, the decay rate of the reconstruction error changes.

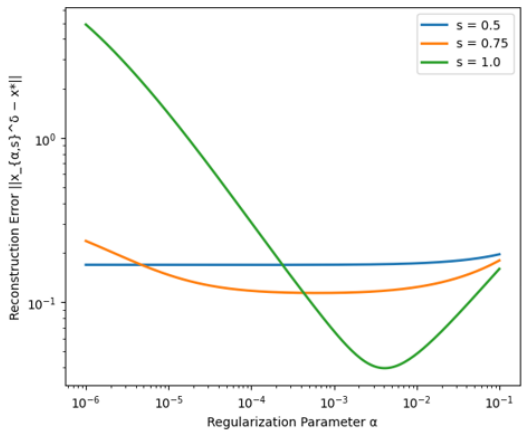

FIGURE 12. Error Decay under Fractional Regularization for Different Orders

In severely ill-posed problems, if the singular values decay exponentially,

$$\sigma_i \asymp e^{-\beta i}, \quad \beta > 0, \tag{4.5}$$

the inverse problem becomes fundamentally more unstable. The best choice of parameters yields convergence at best logarithmically,

$$\mathcal{E}(\alpha_\delta, \delta) \asymp | \log \delta |^{-\gamma}, \tag{4.6}$$

which describes limitations imposed by information theory rather than the regularization technique employed. This effect is demonstrated in Figure 13.

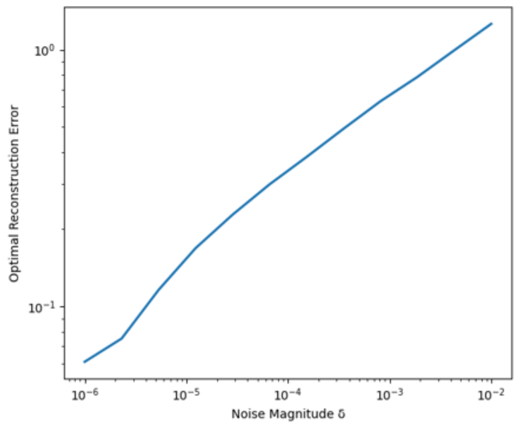

FIGURE 13. Saturation Phenomenon: Error vs Noise Level in Severe Ill-Posedness

Table 2 integrates the main strategies of parameter choice and the related theories of sufficiency, contrasting a priori scaling laws with a posteriori strategy such as the discrepancy principle and the L-curve criterion.

Table 2. Parameter Choice Rules and Their Theoretical Guarantees

Rule	Criterion	Guarantee
Discrepancy Principle	$\| Ax_\alpha^\delta - y^\delta \| = \tau\delta$	Strong convergence
L-Curve Criterion	Maximum curvature	Empirical convergence
Balancing Principle	Bias≈ stability	Scaling law
Quasi-Optimality Principle	Minimize successive difference	Conditional convergence
Generalized Cross Validation (GCV)	Minimize predictive risk	Mean-square convergence
A priori Rule	$\alpha \asymp \delta^{1/(\mu+\nu)}$	Optimal convergence rate

5. Conclusion

In this research, a singular operator-theoretic framework has been proposed for the analysis of regularization techniques used for resolving ill-posed linear operator problems in Hilbert spaces. Beginning with the compact equation $Ax = y$, the analysis showed that the ill-posedness of such equations resides in the spectral decay $\sigma_k \to 0$, which alters bounded invertibility and makes the formal inverse unstable. It was illustrated, via singular system representation, that instability is a product of the amplification components σ_k^{-1} due to small singular values. Encapsulated in the form of $x_\alpha^\delta = R_\alpha y^\delta$, regularization was seen as a means of spectral modification of the operator, incorporating stabilization into the functional calculus applied to A^*A. This operator-theoretic perspective provided a coherent way to analyze instability, approximation, and noise. Unified representations for spectral filters were developed for Tikhonov regularization, truncated singular value decomposition, and iterative polynomial filtering. Each method was developed to replace the unstable factor σ_k^{-1} with a bounded filter function $g_\alpha(\sigma_k^2)\sigma_k$, which suppresses high-frequency amplifications. For the reconstruction error, the structural decomposition $\| x_\alpha^\delta - x^\dagger \| \leq \| (I - R_\alpha A)x^\dagger \| + \| R_\alpha(y^\delta - y) \|$ illustrated the bias-variance decomposition that affects the regularization process.

In the mildly ill-posed regime, polynomial spectral decay for the convergence rate demonstrated that the optimal parameter balancing produced algebraic convergence rates like $\| x_{\alpha(\delta)}^\delta - x^\dagger \| \asymp \delta^{\mu/(\mu+\nu)}$, linking reconstruction accuracy to the smoothness of the exact solution and the decay behavior of the forward operator. The investigation also clarified that regularization design cannot be disentangled from parameter choice theory. The optimal parameter is achieved by balancing approximation and perturbation, leading asymptotically to $\alpha_{opt} \asymp \delta^{1/(\mu+\nu)}$, a relationship that forms the basis of both a priori scaling laws and adaptive rules, including the discrepancy principle $\| Ax_{\alpha_\delta}^\delta - y^\delta \| = \tau\delta$. Geometric choice methods such as the L-curve method were seen as concrete instances of this balancing mechanism. Thus, parameter choice is not merely a computational device, but an essential element of convergence theory.

The research further considered fractional spectral regularization and showed that stability is maintained while approximation behavior can be improved through continuously adjusted qualification order. However, in the extremely ill-posed case, where exponential spectral decay $\sigma_k \asymp e^{-\beta k}$ is present, a logarithmic convergence barrier $\| x_{\alpha(\delta)}^\delta - x^\dagger \| \asymp | \log\delta |^{-\mu}$ remains, reflecting an intrinsic saturation behavior that does not depend on the particular filter. This shows that the spectral structure of the forward operator determines the ultimate limit of regularized reconstruction. Overall, the work integrates spectral theory, regularization design, parameter choice, and asymptotic convergence into a single Hilbert-space framework for inverse problems, while also indicating future scope for nonlinear inverse problems, adaptive multi-parameter regularization, and data-based spectral filtering in infinite-dimensional settings.

References

[1] Clason, C. (2020). Regularization of inverse problems. arXiv preprint arXiv:2001.00617.

[2] Zhang, Y., Hofmann, B. (2020). Two new non-negativity preserving iterative regularization methods for ill-posed inverse problems. arXiv preprint arXiv:2002.04474.

[3] Bortolotti, V., Landi, G., Zama, F. (2025). Uniform multipenalty regularization for linear ill-posed inverse problems. SIAM Journal on Scientific Computing, 47(2), A790-A810.

[4] Jin, Q. (2024). On saturation of the discrepancy principle for nonlinear Tikhonov regularization in Hilbert spaces. Applied Mathematics Letters, 156, 109150.

[5] Kavitha, M. (2025). Hybrid AI-mathematical modeling approach for predictive maintenance in rotating machinery systems. Journal of Applied Mathematical Models in Engineering, 1(1), 1–8.

[6] Yu, S., Yang, H. (2024). Regularization with two differential operators and its application to inverse problems. Applied Numerical Mathematics, 201, 129-144.

[7] Hauptmann, A., Mukherjee, S., Schönlieb, C. B., & Sherry, F. (2025). Convergent regularization in inverse problems and linear plug-and-play denoisers. Foundations of Computational Mathematics, 25(4), 1087-1120.

[8] Namrata Mishra. (2026). Advanced Spectral and Statistical Learning Methods for Intelligent Interpretation of Non-Stationary Signals. Transactions on Advanced Signal Processing and Analytics, 1(1), 38–45.
[9] Mathé, P., Hofmann, B. (2025). Comparing the ill-posedness for linear operators in Hilbert spaces. Advances in Operator Theory, 10(2), 36.
[10] Surendar, A. (2025). Hybrid LLM-algorithm optimization: iterated fine-tuning for combinatorial problems. Frontiers in Mathematical and Computational Research, 32-39.
[11] T. Senthil, "Translating Theory into Practice: A Multidisciplinary Framework for Addressing Complex Real-World Challenges", Bridge: Journal of Multidisciplinary Explorations, vol. 1, no. 3, pp. 34–40.
[12] Dykes, L., Kuian, M., Mach, T., Noschese, S., Reichel, L. (2025). Solution of linear ill-posed operator equations by modified truncated singular value expansion. Journal of Computational and Applied Mathematics, 467, 116621.
[13] George, S., Sadananda, R., Padikkal, J., Kunnarath, A., Argyros, I. K. (2024). New Trends in Applying LRM to Nonlinear Ill-Posed Equations. Mathematics, 12(15), 2377.
[14] N. Arvinth, & David Gichoya. (2025). A Scalable Reconfigurable Processor Architecture for Heterogeneous Edge Computing Applications.SCCTS Transactions on Reconfigurable Computing, 3(2), 40-48.
[15] Hurault, S. (2023). Convergent plug-and-play methods for image inverse problems with explicit and nonconvex deep regularization (Doctoral dissertation, Université de Bordeaux).
[16] Beraldo, R. G., Ferreira, L. A., Suyama, R. (2025, September). Regularization for Inverse Problems and Machine Learning: A Tutorial. In 2025 38th SIBGRAPI Conference on Graphics, Patterns and Images (SIBGRAPI) (pp. 1-6). IEEE.
[17] Nair, M. T. (2021). Regularization of ill-posed operator equations: an overview. The Journal of Analysis, 29(2), 519-541.
[18] Sadaghiyanfam, S., Kamberaj, H., Isler, Y. (2025). Predicting Ionic Liquid Toxicity with Graph Attention Networks. Akıllı sistemler ve uygulamaları dergisi, 25-35.
[19] Singh, H. (2022). Regularizing An Ill-Posed Problem with Tikhonov's Regularization.
[20] Nisha Milind Shrirao, Nidhi Mishra. (2025). Terabit-per-Second Photonic Nanoelectronic Devices for Data Center Interconnects. tProgress in Electronics and Communication Engineering, 3(1), 73-79.
[21] Bakushinsky, A. B., Kokurin, M. M., Kokurin, M. Y. (2018). Regularization algorithms for ill-posed problems (Vol. 61). Walter de Gruyter GmbH and Co KG.
[22] Krnst Beken, Hardley Caddwine. (2026). Data-Efficient Learning-Assisted Predictive Control for Real-Time Trajectory Planning Under Dynamic Constraints. Journal of Scalable Data Engineering and Intelligent Computing, 17-23.
[23] Kim, S., Rim, B., Choi, S., Lee, A., Min, S., Hong, M. (2022). Deep learning in multi-class lung diseases' classification on chest X-ray images. Diagnostics, 12(4), 915.
[24] Vimala, D. (2026). Integrating mathematical literacy and language development: A curriculum innovation framework for secondary education. Journal of Mathematics, Language and Curriculum Innovation, 2(1), 1–6.
[25] K. Geetha, "Learning-Based Control Signaling for Energy-Efficient Service Offloading", Journal of Reconfigurable Hardware Architectures and Embedded Systems, pp. 18–26.
[26] S. Praveen Kumar. (2026). Algorithm–Architecture Co-Design of High-Throughput DSP Hardware Accelerators for Next-Generation Embedded Systems. Journal of Integrated VLSI and Signal Processing, 1(1), 26–34.

Dr. B. Bhaskar Reddy works as a professor in the ECE department at K.S.R.M. College of Engineering, Kadapa. He graduated in Electronics and Communication Engineering from KSRMCE, S.V. University, Tirupathi, and secured his M.E. Degree from TCE, Madurai, under Madurai Kamaraj University. He also holds a PhD degree from S.K. University, Anantapur. With over two decades of teaching experience, he has presented numerous papers in national and international symposiums and journals. His main areas of interest include communication, signal processing, image processing, and Internet of Things.

Dr. Raja Kumari Chilukuri was born in Krishna District, Andhra Pradesh, India. She Received her Ph.D. from Koneru Lakshmaiah Education Foundation (Deemed to be University), Vijayawada, Andhra Pradesh, India, in the area of "Radar signal Processing" and the B.E. degree (ECE) from Anna University, the M.Tech. degree from Dr. M.G.R University, Tamil Nadu, India. She received university first rank in the PG Study. She is also a recipient of gold medal in the PG Study. Presently she is working as an Assistant Professor in the Department of Electronics and Communication Engineering, VNRVJIET. She has published Nine international journals and seven conferences. She is a Reviewer for few national and international journals. She has 17 years of teaching experience. Her research interests include Radar signal processing, Microwave, Antennas, Electromagnetic theory and RF. She is a life member of ISTE, IEI, and IAENG. She is also a member of IEEE.

AnilChowdaryTummala(FIETE)completedhisbachelor's degree in Electronics and Communication Engineering with a specialization in 2002 from the Institution of Electronics and Telecommunication Engineers, New Delhi. He further pursued his master's degreewithaspecialization inVLSIDesignfromS.R.M.University- Chennai, INDIA in 2005. His research passions encompass Video, Image, and Signal Processing, with an emphasis on their implementationusingFPGA,ASIC,andSoCtechnologies,alongwith NoC integration. He was awarded with Ph.D. from VIT-AP University's School of Electronics Engineering in INDIA, where he continuestocontributetoadvancementsinthesefields.Currently, he is working as an Associate Professor at SRK Institute of Technology, INDIA.

Venkateswara Rao Musala, born in Vijayawada, AP, India, is an Associate Professor in the Electronics and Communication Engineering Department at Dhanekula Institute of Engineering and Technology, Vijayawada , India. His qualifications include M.Tech in VLSI Design from Sathyabama University, Chennai. MTech and PhD from KL University Vijayawada. With a focus on teaching and research. His research interests include SoC, FPGA, Hardware Accelrators, Quantum Computing.

Hari Kishore Kakarla,born in Vijayawada, AP, India, is a Professor in the Electronics and Communication Engineering department at KL University, Guntur. His qualifications include B. Tech (ECE) from JNTU Hyderabad, MTech from SKD University Anantapur, and PhD from KL University Vijayawada. With a focus on teaching and research, he's a Life Member of ISTE and has published 145 international journals and 12 International Conferences.

Dr. Kavitha Manoharan is a distinguished academic and researcher currently affiliated with the Saveetha School of Engineering in Chennai, India. With a robust research portfolio and an h-index of 6, she has established herself as a significant contributor to the fields of electronic engineering, telecommunications, and intelligent systems. Her scholarly work is characterized by its technical depth and interdisciplinarity, spanning from foundational VLSI design and leakage current reduction in SRAM to advanced AI governance architectures. To date, she has published 16 documents indexed in Scopus, which have garnered over 140 citations from the global research community, reflecting the practical impact of her work on modern engineering challenges.